

ON THE USE OF SATELLITE DERIVED HEATING RATES TO INITIALISE TROPICAL FORECASTS

William A. Heckley, Graeme Kelly and Michael Tiedtke
European Centre for Medium Range Weather Forecasts
Shinfield Park, Reading

Abstract

The HIRS instrument on the NOAA polar orbiting satellites is used to obtain coverage of OLR across the global tropics and subtropics four times a day. From this is obtained fractional coverage of cold cloud, which is then interpreted as rainfall rates. This information is introduced into the ECMWF data assimilation system as diabatic heating through the non linear normal mode initialization scheme. Substantial impact on the analyses is found.

1. INTRODUCTION

Analysis systems as used to provide initial conditions for numerical weather forecasts usually seek to blend observations together with a background field in a statistically optimum and multivariate manner. The exact form this takes varies. In all cases, however, the success of the technique depends on the quality of the background field, the coverage and quality of the observations, and a knowledge of the statistical structure of the errors in the background field and in the observations. At ECMWF the background field is a six hour forecast from the previous, initialised, analysis. For a useful review of current practice in objective analysis for numerical weather prediction see Hollingsworth (1986).

In the northern hemisphere extratropics this approach works well. The background field is fairly accurate, of comparable accuracy to the observations, and its error structure can be determined (Hollingsworth et al., 1985). With the notable exception of the Pacific, there is a good coverage of observations.

Within the tropics the situation is quite different (Shaw, 1984). Near the equator there exists no simple relationship between mass and wind fields, making any form of multivariate analysis difficult. The analysis scheme has to become univariate near the equator. Subsequent adjustment can be through variational schemes (e.g. Jones, 1976), model adjustment (e.g. Lyne et al., 1982) or through initialisation. The weak pressure gradients in the tropics present difficulties in that observing techniques frequently lack sufficient accuracy to resolve the gradients, inaccurate observations may frequently degrade rather than enhance the analysis. Lack of high quality mass observations also leads to aliasing

between large scale Rossby and Kelvin modes (Cats and Wergen, 1983). Perhaps the most serious problem for tropical analysis is the lack of data. Paucity of data leads to far greater uncertainty in the analyses than occurs in the northern hemisphere extratropics, with the possibility of serious deficiencies in the background field being uncorrected by the analysis. This, in turn, implies difficulties in quality control of data. It is clear that the quality of the tropical analyses will depend crucially on the quality of the background field and of the model used to produce it. Inadequate parametrization of physical processes can lead to large errors in the tropical forecasts and these can have a significant effect on the analyses (Tiedtke et al., 1988, Hollingsworth et al., 1988).

The general lack of 'conventional' data in the tropics, leads to a need to utilise as much information as possible from the meteorological satellites. For reasons alluded to above the most important quantity is that of wind. This is deduced from satellite imagery through the expedient of tracking clouds between subsequent cloud images. This technique has many limitations. It is usually only possible to obtain clouds at one, or at most two, levels (usually about 800 or 250 hPa). Problems include, determination of the cloud top height (knowing at precisely which level to assign the wind); uncertainty as to whether it is the same cloud that is being tracked from one frame to the next; and clouds are not simply just advected along with the environmental flow at that level (Källberg, 1985). Apart from these problems, rarely is there enough of these cloud track winds processed in order to clearly define the divergence field at either of these levels.

It is observed that, within the tropics, deep, cold clouds are usually associated with low level inflow, upper level outflow, and precipitation. This observation has led to satellite imagery being used in more direct ways to analyze the divergence field, e.g. through empirical relations between OLR and divergence (Julian, 1984; Krishnamurti and Low-Nam, 1986). Kasahara et al. (1988) empirically relates the strength of the vertical (ω) velocity to the OLR temperature (when this temperature is less than a threshold value), then, assuming a parabolic profile for ω , calculates the divergence field from continuity.

Information provided by visible and/or infrared imagery regarding the spatial and temporal distribution of cloud top temperature and cloud brightness has been used to deduce the intensity of precipitation at the surface beneath these clouds. A review of such techniques can be found in Barrett and Martin (1981).

A rainfall analysis from satellite imagery can be enhanced through combining this information with synoptic observations from rain gauges e.g. Krishnamurti et al. (1983).

Such analyses have been used to deduce the omega field through matching deduced rainfall rates with the model's parametrization of deep convection (Krishnamurti et al., 1984).

In view of the dominant role of diabatic processes within the tropics, and also the general lack of conventional data, it makes sense to utilise more direct measures of the diabatic forcing within the assimilation. Puri (1987), working with the ECMWF model, has used OLR to specify heating rates, which are then used in diabatic non-linear normal mode initialisation of the analyses. A major limitation of his study is in the data source available for the OLR, which was twice daily, at a resolution of 2.5 degrees. Specifically, to be of use within the analysis, it is necessary to have an idea of the quality (data coverage) and time of each observation, point by point; and ideally to provide global fields every six hours. Also as it turns out, OLR in itself does not provide a sufficiently good measure of precipitation.

Use of the satellite imagery through the initialisation does not preclude its use in other ways such as those referred to earlier, indeed it could be argued that for consistency one should try to use the information both through analysis and initialisation.

Another motive for using 'diagnosed' heating rates in the initialization is that the model suffers from a spin-up problem (Girard and Jarraud, 1982; Heckley, 1985), in which during the first few hours of a forecast the predicted values of condensed water and, therefore of latent heating, are too small, particularly in the tropics. As pointed out by Kasahara et al. (1988) this problem appears to some extent in all forecast models, and is one of the unsolved problems in numerical weather prediction. Solutions have been attempted through modification of the initial divergence and/or moisture field, such as those mentioned earlier; initialization of cumulus convection (Donner, 1988; Donner and Rasch 1990); and through dynamic relaxation (Krishnamurti et al., 1988). These have met with varying degrees of success. Recent experience with the ECMWF model using other parametrizations of cumulus convection show different behaviour, in that some schemes exhibit spin-up in which the initial convection is too large. The problem remains that the convection is initially wrong, either too intense or too weak. For an operational forecasting model, spin-up remains an unsolved problem. It has been shown by Mohanty et al. (1986) that diabatic nonlinear normal mode initialization (NNMI) schemes using model generated heating rates retain far less intensity of analyzed divergence than does the use of NNMI with diagnosed heating rates. In this case the diagnosed heating rates were determined as a residual of the thermodynamic energy balance using analyzed synoptic data. Since the determination of the heating requires prior knowledge of the predicted fields this technique is not applicable to operational forecasting.

2. PRECIPITATION ANALYSIS

The NOAA series of orbiting satellites carry, as part of their instrument package, a High resolution Infrared Radiation Sounder (HIRS) sampling 20 channels from .7 to 15 micron. Each measurement resolves a circular area of 30 km diameter at the satellite sub-point and there are 56 fields of view within each scan. Each scan covers approximately 2250 km on the earth's surface and is perpendicular to the satellite track. A more detailed description of the TIROS-N system may be found in Smith et al. (1979). At any one analysis time between five and ten orbits are available from a combination of the NOAA9 and NOAA10 space craft, providing typically around 500000 observations globally. Fig 1 shows the coverage of the HIRS data within +/- 3 hours of 12 UTC 2/2/87. Typically, coverage is such that at each of the main synoptic hours there are few data voids.

A number of known atmospheric profiles have been input to a forward radiation model to calculate both the total long wave radiation (OLR) and the first 12 HIRS channels. From these calculations a set of regression equations have been determined. These regressions are then used to estimate OLR at each HIRS spot. The calculations are performed using code obtained from 'The Physical Retrieval TOVS Export Package' Smith et al.(1984). Values of OLR are converted to brightness temperature. For each spot there is then available the temperature and the time of the observation. In the case of overlapping orbits, data from the orbit closest to the analysis time is used, coincident data from other orbits is discarded. Spots are collected into 7*7 boxes and the fractional coverage of cold cloud is calculated within each box by counting the number of spots colder than 235 K. The result is an estimate of the fractional coverage of cold cloud at a reduced resolution of about 2.5 degrees. The value 235 K was chosen as it was found by Richards and Arkin (1981), and by Arkin (1979), to be the optimum threshold for estimating convective rainfall within 2.5 degree boxes.

A Cressman analysis is now carried out both of the fractional coverage of cold cloud and of the observation times. This is done on a regular grid which is close to the model's Gaussian grid. It has a resolution of 1.121 degrees in the north-south and 1.125 degrees in the east-west. Five passes are used in the Cressman analysis, with north-south radii of 9.1, 5.1, 2.5, 1.5, and 1.1 grid points, respectively. In the east-west the radii are those of the north-south, divided by cosine of latitude - thus more east-west points are used as one moves away from the equator. A check is made between each pass to eliminate negative values. Smoothing, basically a two-grid length filter, is carried out on the second and fourth passes. In the case of the analysis of fractional coverage of cold cloud a first guess field that is zero everywhere is used as input to the Cressman analysis. The effect of the various passes can be seen in the analysis of data times, an example of which is shown in Fig 2 (for 12 UTC 2/2/87). Note that the analysis of the observation times is expressed as

Location of HIRS data, Date: 870202
Within +/- 3 hours of 12 UTC

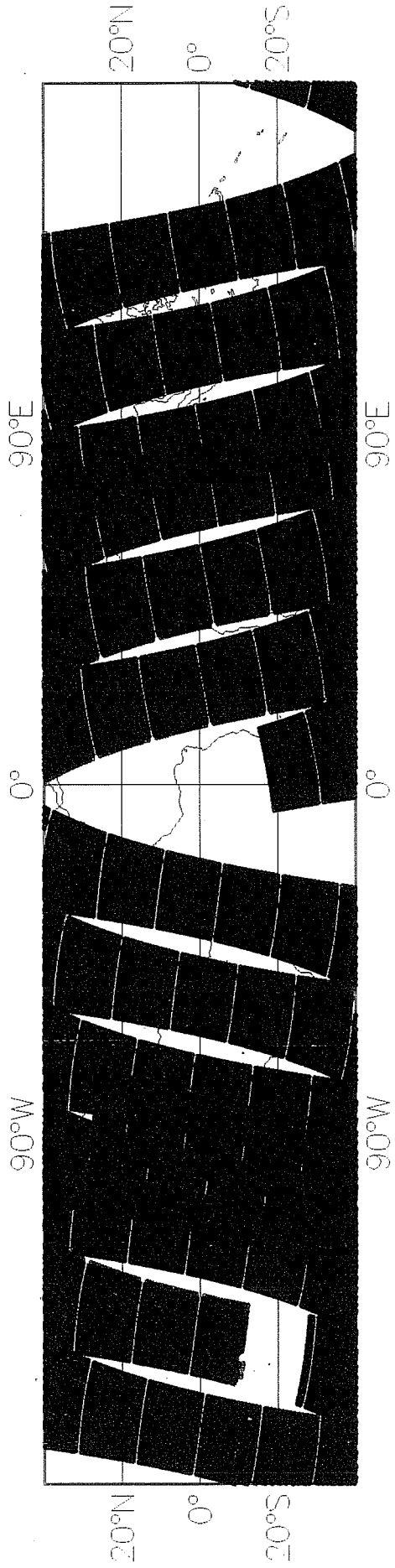


Fig 1. Location of HIRS data within +/- 3 hours of 12 UTC 2/2/87.

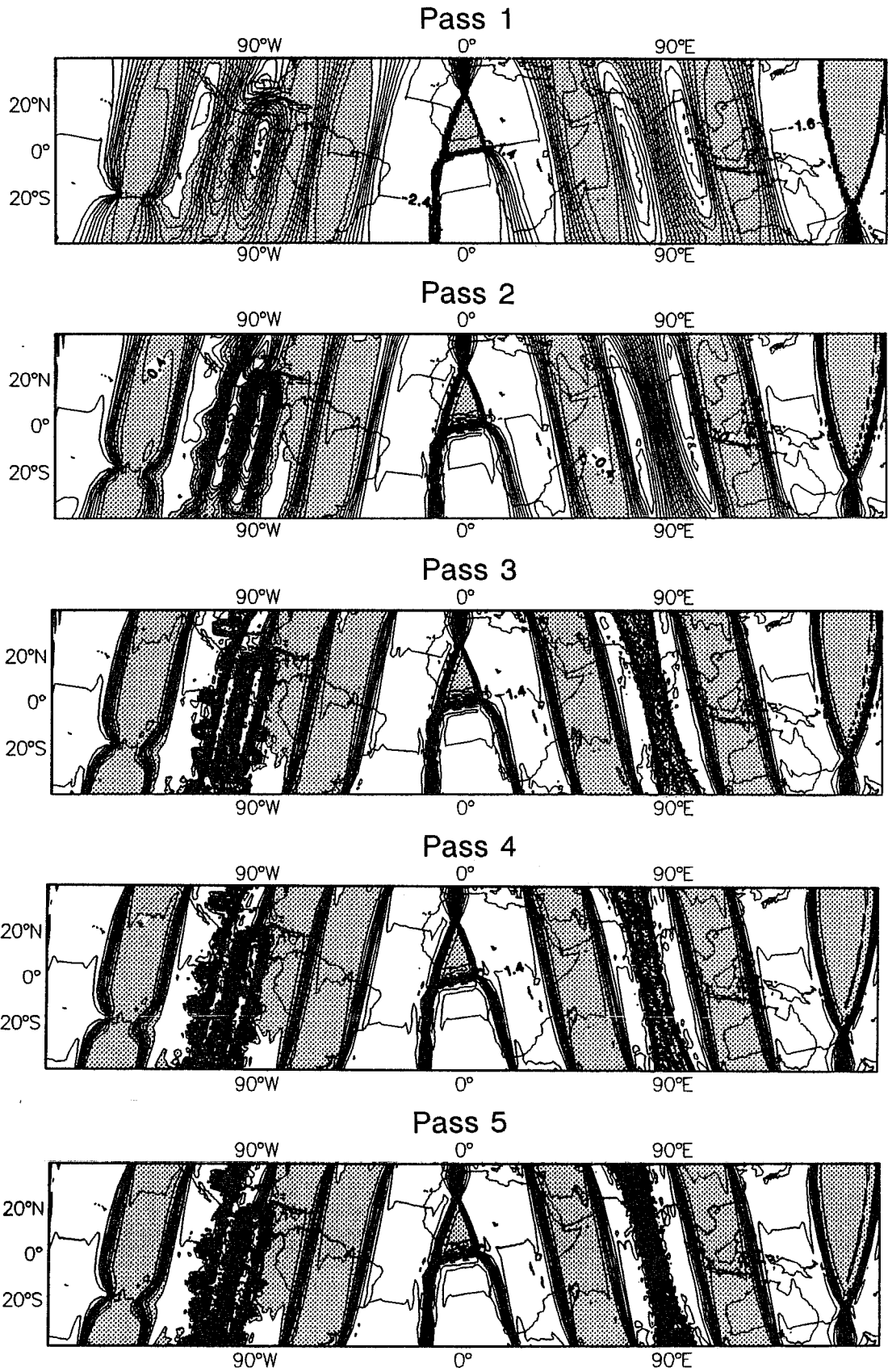


Fig 2. Analysis of the departures of observation times from analysis time (12 UTC 2/2/87). Areas in which observations are within +/- 1 hour of the analysis time are shaded.

departures from the analysis time. Thus - 1.6, for example, indicates 1.6 hours prior to the analysis time (12 UTC). Shaded areas indicate regions in which the observations are within one hour of the analysis time. The broad first passes are used to fill in the gaps between close orbits, consecutive passes fill in the details.

A by product of the Cressman analysis is a field of weights which can be regarded as a point by point measure of the data density. Following the analysis, the weights (taken from the first pass) are rescaled to be between zero and one, in order to provide confidence limits for the analyses. Fig 3a shows an example of these 'confidence weights' for 12 UTC 2/2/87, cf Fig 1. The analysis of observation times, Fig 2, is used to modify the field of confidence weights (fig 3a) in such a way that the weights are progressively reduced according to the degree of asynopticity of the data. A factor of the form

$$\exp(-0.057 \times (t - t_a)^2),$$

is used. Where t is the observation time and t_a is the analysis time. This has the effect of reducing the weights by a factor of two when $(t - t_a)$ is about 3.5 hours. Such an analysis is shown in Fig 3b, again for 12 UTC 2/2/87.

Finally the weights are subjected to a latitudinal weighting such that they become zero poleward of 35 degrees and can only reach their maximum value equatorward of 25 degrees. Between 25 and 35 degrees the weights are further modified by a factor

$$\sin((35 - \text{lat}) \times \pi \times 0.05),$$

as shown in Fig 3c. Thus the field of weights now reflects the data distribution, the asynopticity of the observations and air mass type.

Arkin and Meisner(1987) define a GOES Precipitation Index (GPI). The GPI is calculated as the product of the mean fractional coverage of cloud colder than 235 K in a 2.5 x 2.5 degree box, the length of the averaging period in hours and a constant of 3 mm/hour. That is

$$\text{GPI} = 3F_c t.$$

Following the work of Arkin and Meisner(1987), the precipitation rate is defined here as

$$\text{precipitation rate} = 3F_c.$$

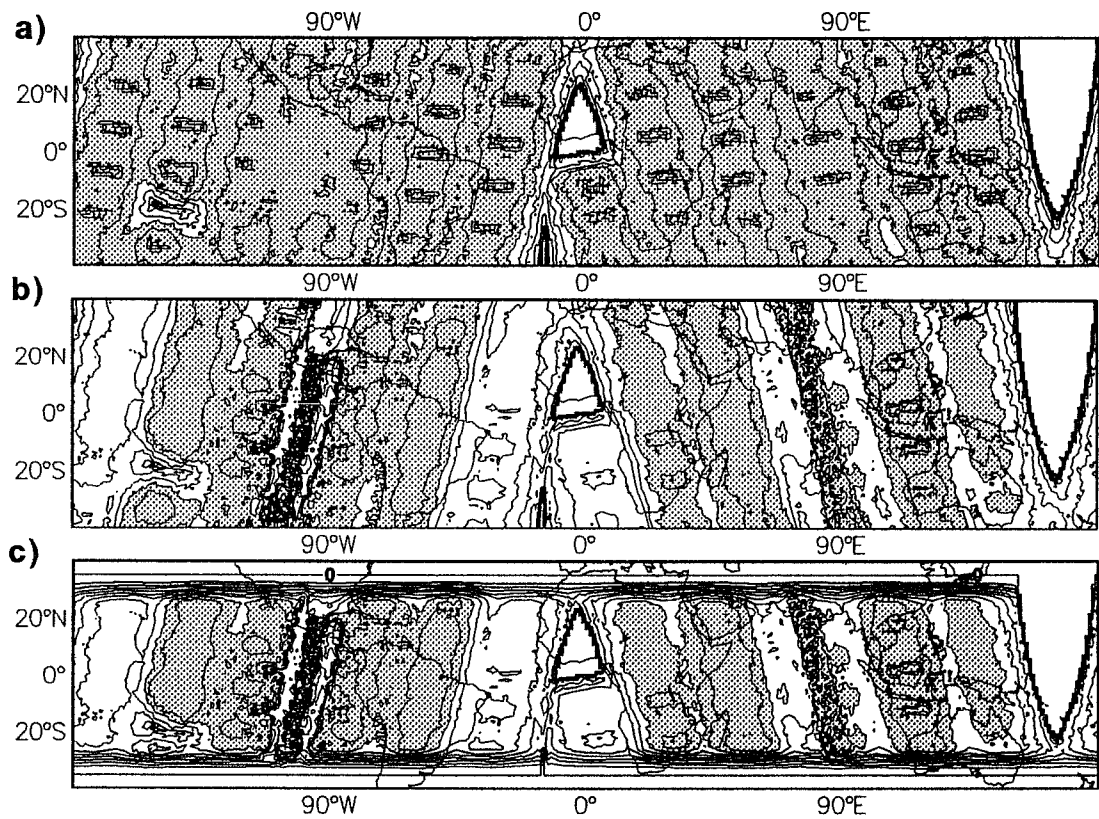


Fig 3. Field of analysis weights, a) unmodified; b) modified by the degree of asymptoticity of the data; c) modified as b) and also by latitude. Contour interval is 0.1. Values greater than 0.8 are shaded.

The precipitation rate is the quantity which will be used within the initialisation. For the purposes of plotting it is converted to precipitation amounts by multiplying by 24 to obtain a daily total. This should be interpreted with care since it is unlikely that the precipitation rate persists unchanged for 24 hours. An example of the precipitation analysis is shown in Fig 4a for the tropical belt, and in figs 4b and 4c for South America and Australasia respectively, all are for 12 UTC 2/2/87. Comparison with the weights in Fig 3a suggests that the lack of precipitation around 170°E is most likely due to there being a data void in this region at this time. Climatologically (e.g. Jaeger, 1976) the distribution of the diagnosed precipitation in Fig 4a looks reasonable. Looking in more detail at Figs 4b, 4c, the geographical spread of the precipitation would seem to be too large for precipitation rates over 6 hours.

The GPI index of Arkin and Meisner (1981) is a relation derived from GATE data, which applies to precipitation from easterly waves in the eastern tropical Atlantic. Further, it was derived from geostationary satellite imagery, and intended for producing precipitation estimates for periods of about two weeks, by averaging the OLR over that period. In this study the relation is used to provide an estimate of instantaneous precipitation rates from polar orbiting satellites, over the global tropics and sub-tropics. As such it can only be regarded as a qualitative measure of the location and amounts of precipitation. However due to the way this information is to be used this is sufficient for this study.

3. USE WITHIN THE ASSIMILATION

The data assimilation scheme used at the ECMWF is an intermittent four dimensional scheme (Bengtsson et al., 1982), in which a global multivariate analysis (Shaw et al., 1987, Lorenc, 1981) is carried out at intervals of six hours. A first guess is used for the analysis which is a six hour forecast from the previous, initialised, analysis. This forecast uses the same model as that used to undertake medium range forecasts (Simmons et al., 1989; Tiedtke et al., 1979; Tiedtke et al., 1988; Miller et al., 1989). Initialisation is necessary in order to prevent spurious noise in the six hour forecasts which would otherwise cause problems with quality control of observations in the subsequent analysis.

A non-linear normal mode initialisation scheme is employed (Machenhauer, 1977), as described by Wergen (1988, 1989), and Wergen and Heckley (1987). Diabatic processes are included as a constant term in the iterations of the initialisation. Holding them constant in this way circumvents convergence difficulties otherwise induced by these terms. The diabatic forcing is obtained from an integration of the forecast model from the uninitialized analyses, the first two timesteps are ignored (due to the rapid adjustments which take place at the start of the forecast), the physical forcing is then time averaged over the next two hours of integration. This forcing is then filtered by projection onto the normal modes.

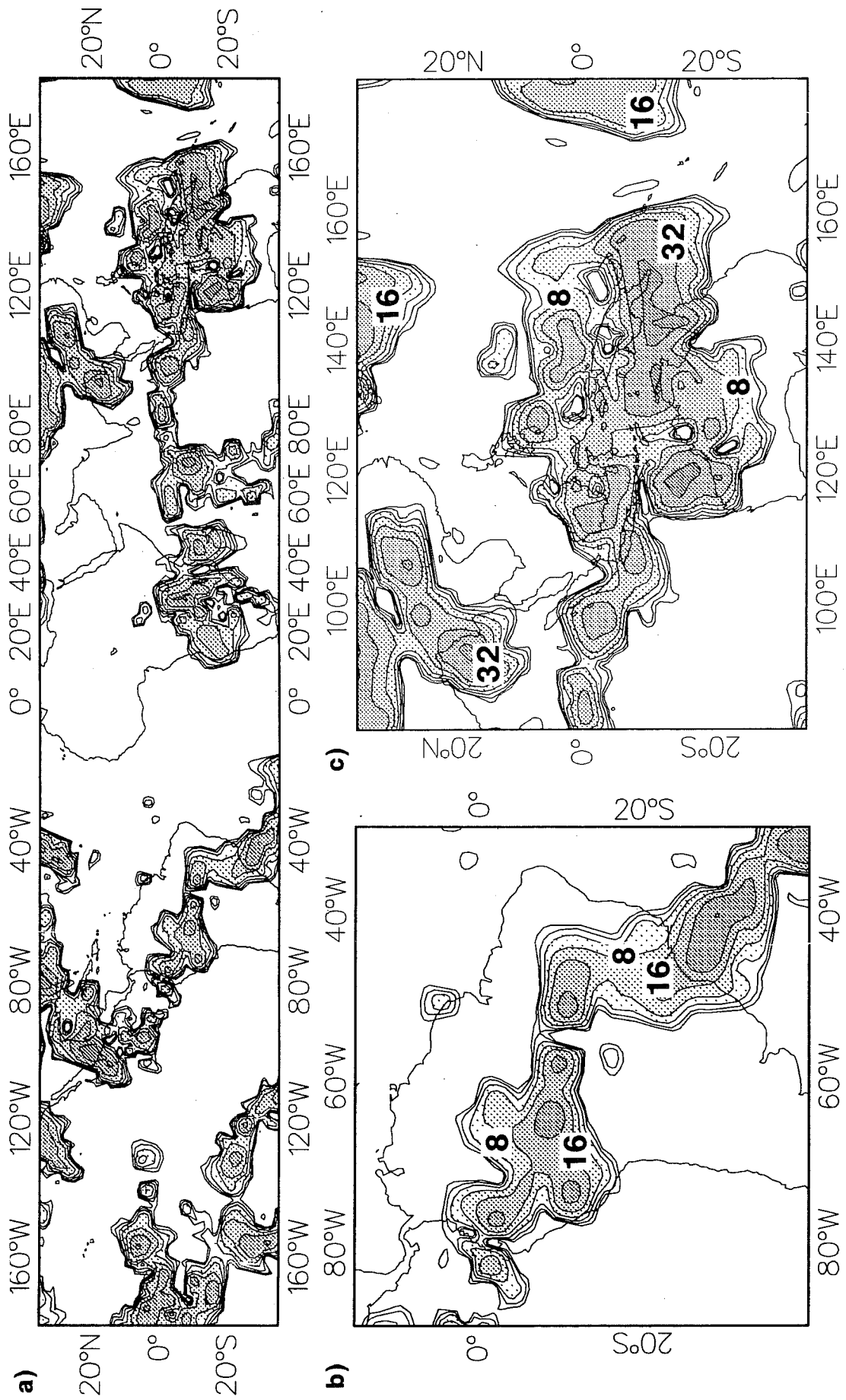


Fig. 4. Analysis of precipitation rates a) global tropics; b) South America; c) Australasia. Contours are at values of 1,2,4,8,16,32,64 mm/day. Values above 4 mm/day are shaded.

Only the large scale component (within the first twenty zonal and twenty meridional modes) of the projection onto the 'slow' gravity modes is retained. Slow in this case means modes whose free period is five hours or larger. Because of the nature of the gravity modes, the frequency constraint also acts as a strong spatial filter on the forcing. The physical forcing thus calculated will be underestimated within the tropics due to the dominance of convective heating in those regions, and the spin up of the model's convective heating (Heckley, 1985), which is initially too weak. However, inclusion of diabatic processes in this way considerably improves analysis of the tropical divergent wind field in the tropics and sub tropics. One of the criticisms of the original ECMWF FGGE IIIb analyses was the weakness of the divergent circulations within the tropics (Lorenc and Swinbank, 1984), this weakness was mainly due to the use of an adiabatic form of initialisation.

Since the tropical flow is largely driven by diabatic processes the 'diagnosed' precipitation rates constitute, in principle, a valuable data source. However, rainfall rate is essentially a measure of the integrated heating rate and the vertical heating profile must be deduced in some way. This is best done through the cumulus parametrization applied in the forecast model so as to ensure consistency of analyses and subsequent forecast. The necessary calculations are rather straight forward with the Kuo scheme used in the ECMWF model until May 1989, where the diagnosed precipitation rates are incorporated as follows.

The appropriate input for the Kuo scheme is a moisture convergence into the grid area to produce precipitation but no moistening (moistening parameter $b=0$). Diagnosed values (DIAG) of moisture convergence are merged with the model generated values (MOD) as

$$(1-wts) \times MOD + wts \times DIAG,$$

depending on confidence in the diagnosed precipitation. Similarly the moistening parameter b is set to $(1-wts) \times MODb$, where $MODb$ is the model b parameter. In regions of high confidence the weights (wts) are close to unity, the moisture convergence is defined by the diagnosed precipitation rate and the moistening parameter is set to zero so that all the moisture convergence falls out as rain. Where there is no data, or in the extratropics, or where the data is far from the synoptic time, the weights (wts) will be close to zero and the moisture convergence will be set to its forecast value (MOD), as will the moistening parameter (MODb). Thus the scheme moves smoothly between forecast and diagnosed convection according to the specified field of confidence weights. The Kuo scheme will generate a field which is consistent with both the diagnosed precipitation and the model parametrization.

Fig 5 shows heating rates at model level 11 (about 500 hPa), averaged over two hours of model integration from 12 UTC 2/2/87, for the Australasian region a) prior to filtering and (b) after filtering. No diagnosed heating has been used in this case. Note the 'spotty' nature of the model heating, and the intense local values. This is a region with little spin up. Contrast the heating obtained when diagnosed heating is used in the model, fig 5c shows the heating prior to filtering and 5d after filtering. Fig 6 shows the heating rates at model level 7 (about 200 hPa), the diagnosed heating assimilation has considerably more heating than the model values at this level. Diagnosed heating rates display a well organised and plausible structure. The effect of the filtering is to retain only the large scale information, reducing the local intensities considerably. However, even with the filtered fields (figs 5b,d and 6b,d) there are substantial differences in the heating as diagnosed and generated by the model.

The use of weights in the merging of the diagnosed and model generated heating rates can be seen by comparing Figs 6a, 6c, and 3c. From Fig 3c it is seen that there is a data gap at around 170°E and Fig 4c shows that no precipitation has been analysed. In this region the heating rates in the diagnosed heating assimilation, Fig 6c, are identical to the model generated values, Fig 6a, and there is a smooth transition between the model generated and diagnosed values.

4. EVALUATION OF THE TECHNIQUE

Vertical distribution of the heating is largely controlled by the Kuo scheme. This may not be ideal as the Kuo scheme may not be representing the true profile of the heating, and it is known that NWP models such as that used at the ECMWF are very sensitive to the vertical profile of the heat sources (see for example, Kanamitsu, 1985). Knowledge of the true heating profile would undoubtedly be useful.

Insertion of the heating through the Kuo scheme works relatively well in some regions, notably the tropical Pacific and Indonesia, but fares less well over the equatorial Atlantic where, presumably due to analysis deficiencies, the flow is initially too stable to support deep convection. Here, although the precipitation analysis may indicate intense precipitation, the Kuo scheme finds that the atmosphere is convectively stable, and no convective heating is produced. This is clearly a deficiency which needs to be addressed within the broader context of analysis of temperature and moisture.

A similar problem occurs over the tropical continents where the model exhibits a strong diurnal cycle in convective activity, essentially cutting off the convection at dusk. Observational studies (Gray and Jacobson, 1977), whilst indicating the existence of a significant diurnal cycle in heavy precipitation, suggest that there is little significant

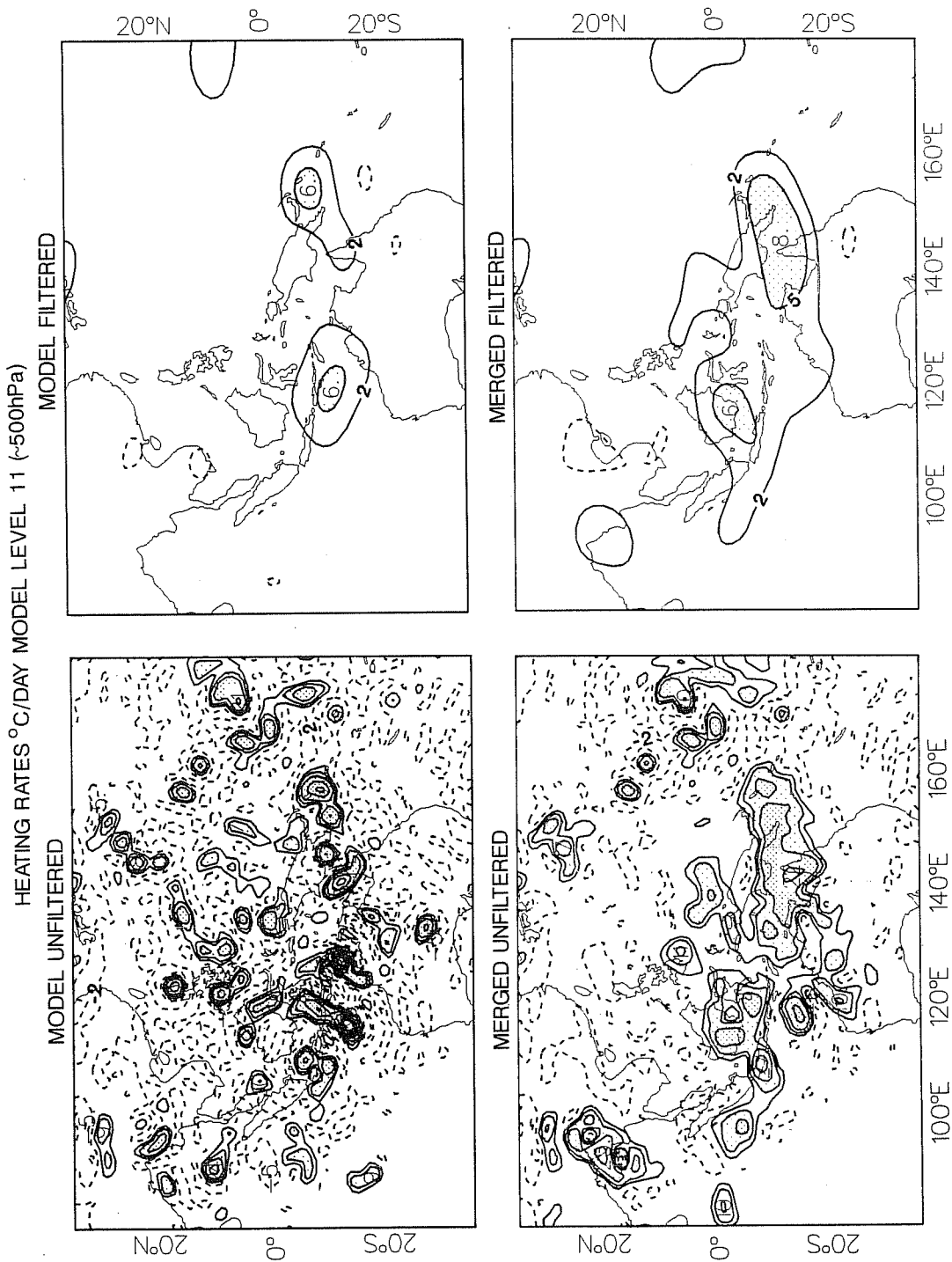


Fig 5. Mean heating rates at model level 11 (about 500 hPa) as averaged over two hours of integration from uninitialised analyses of 12 UTC 2/2/87. Contours are at values of +/- 2,5,10,20,30,40 °C per day. Negative values are dashed.

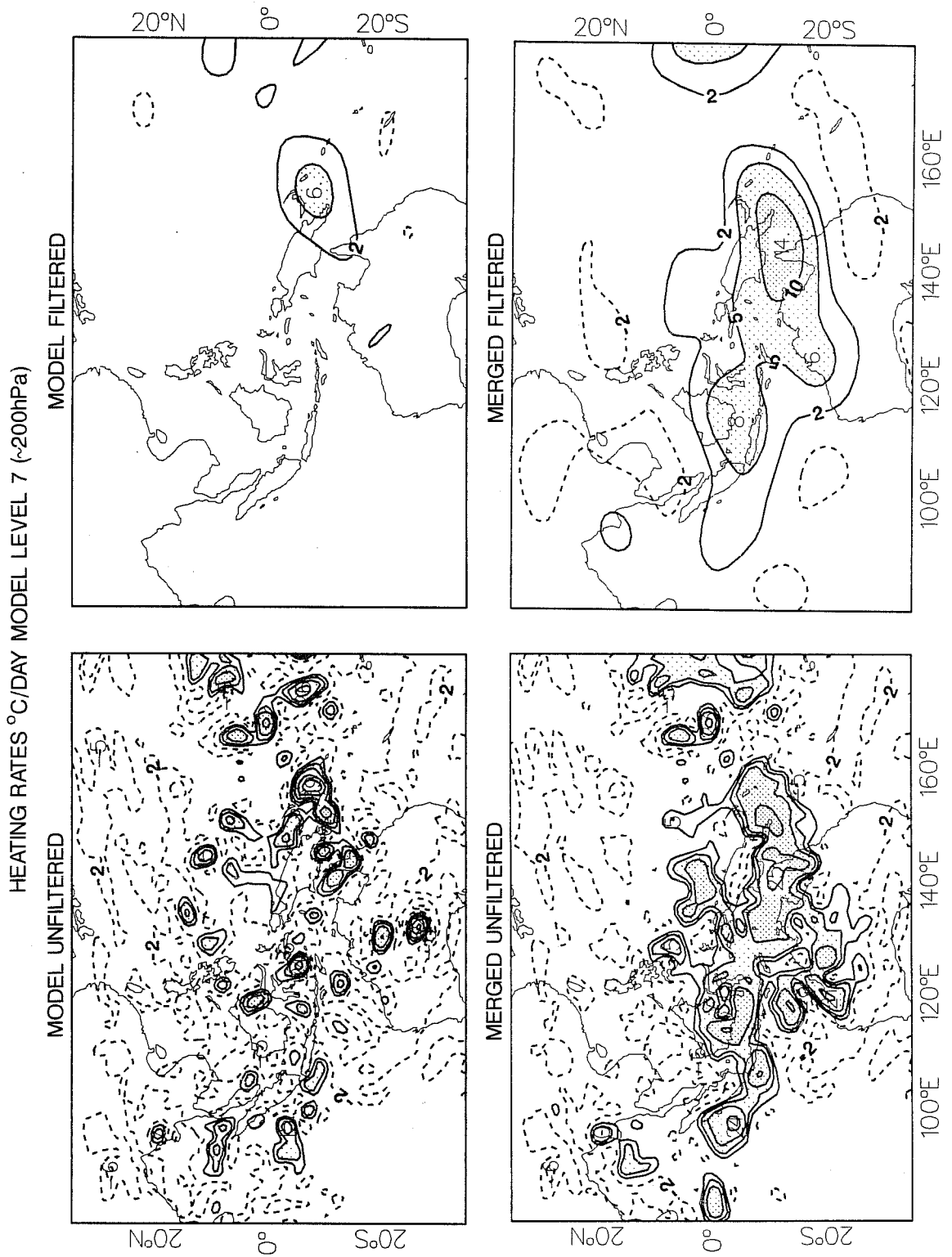


Fig 6. As Fig 5, but for model level 7 (about 200hPa).

diurnal cycle in total precipitation. The diagnosed precipitation rates do not indicate significant diurnal activity, but Gray and Jacobson (1977) point out this is not readily observable from satellite pictures which cannot well resolve individual convective cells. However, due to the problems referred to above, the Kuo scheme finds that the atmosphere is convectively stable at night (over the major tropical land masses) and the diagnosed precipitation is not translated into convective heating. Again, this is an area of further research.

5. ANALYSIS IMPACT

The period chosen for study occurs during the second active period of the Australian monsoon during 1987 (Heckley and Puri, 1988). Three major experiments took place in the north Australian region during this period; the Australian Monsoon Experiment (AMEX, see Holland et al., 1986); the Equatorial Mesoscale Experiment (EMEX); and the Stratosphere-Troposphere Exchange Project (STEP). This involved the establishment of an enhanced radiosonde and SYNOP network. The additional sounding and SYNOP data were transmitted to ECMWF and were included in the data base used to produce the operational ECMWF analyses of this period, although the actual amount received was highly variable. The operational ECMWF analyses for 10/1/87 through 15/2/87, together with satellite imagery and time means over the various active and inactive periods of AMEX have been documented in ATLAS form (Heckley and Puri, 1988).

A data assimilation experiment, with the additional AMEX data referred to above, has been carried out starting from 00 UTC on 1/2/87 through to 12 UTC on 8/2/87, using the version of the forecast model and analysis system current in December 1988. As numerous changes have taken place since February 1987, a control assimilation (without the use of the diagnosed heating) has been carried out for the period 00 UTC on 1/2/87 through to 12 UTC on 2/2/87. This allows evaluation of the assimilation impact over seven analyses, six hours apart. Forecasts have been run from both assimilations from 12 UTC on 2/2/87, these are discussed in the next section.

The overall analysis impact is most clearly seen by averaging over the seven initialized analyses and looking at the differences between the assimilation with diagnosed heating included and the control assimilation. Fig 7 shows the height field differences at a) 200 hPa, and b) 850 hPa. There is clearly an increase in the 200/850 hPa thickness, indicative of a warming, over much of the tropical Pacific; and a decrease in the 200/850 hPa thickness over the Indian Ocean and Indonesia, indicative of a cooling. The warming over the tropical Pacific is to be expected in view of the spin up problems with the model convection in this region, more heating is going into the initialisation with the use of the diagnosed heating. The cooling over the Indian Ocean was less expected. Associated with

ENSEMBLE DIFFERENCE BETWEEN DIAGNOSED HEATING AND CONTROL ASSIMILATIONS

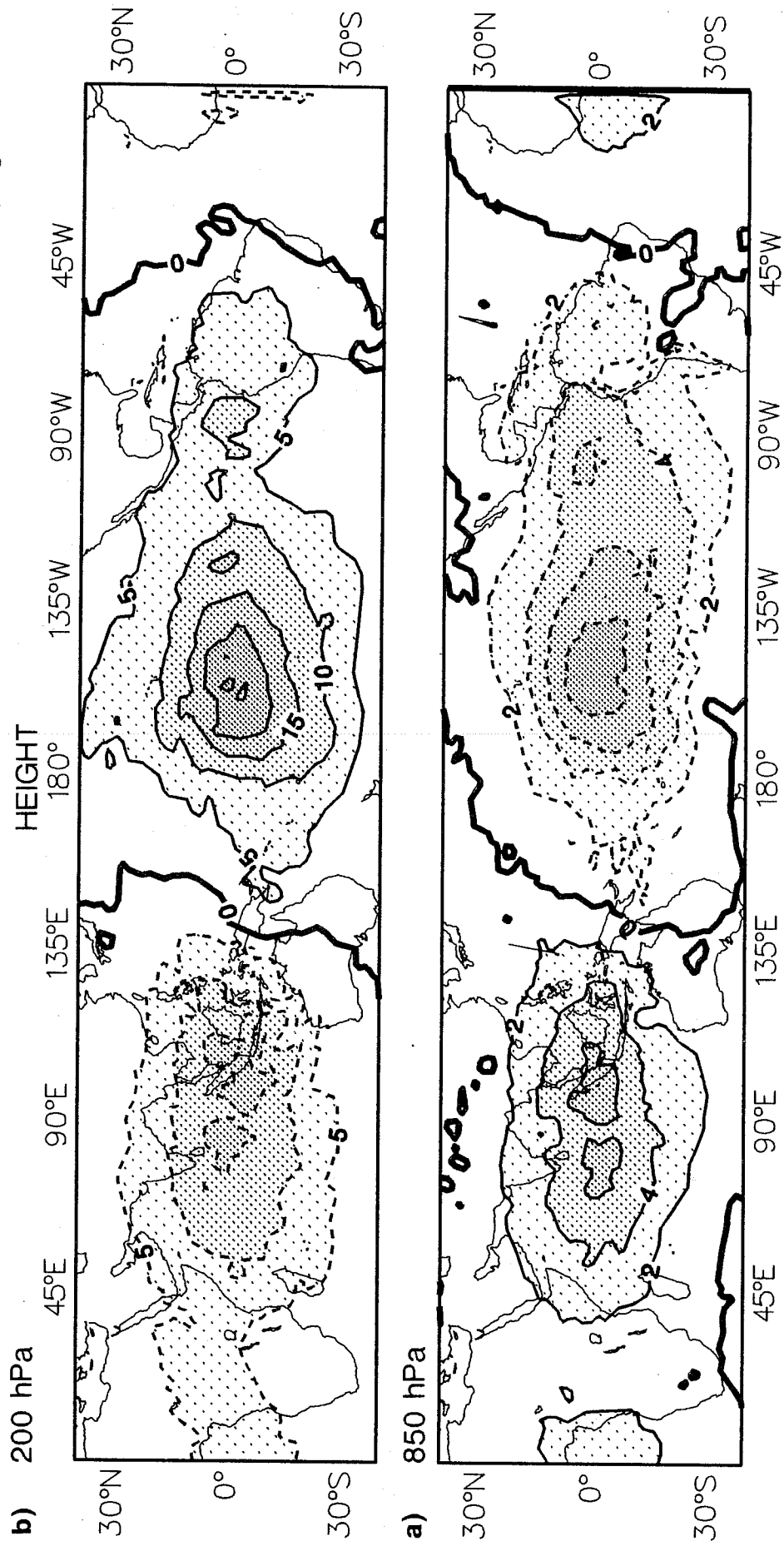


Fig 7. Ensemble difference between diagnosed heating and control assimilations (7 cycles). Height field a) 200 hPa, contour interval 5 m. b) 850 hPa, contour interval 2 m. Negative values dashed.

the changed thermal structure are more intense Hadley and Walker circulations. Fig 8 shows the analysis differences at a) 200 hPa, and b) 850 hPa, in the velocity potential. Fig 9 shows the corresponding streamline fields (contours are isotacs). Interestingly, the largest velocity potential changes occur at longitudes between the main thermal changes (c.f Fig 7), suggesting that horizontal advection is playing an important role, through the first guess forecast. The wind field differences are clearly indicative of an enhanced heat source (see for example, Gill, 1980). Again the large values in the eastern Pacific suggest advection of differences through the first guess forecasts. Differences in the rotational component of the wind are largely concentrated in data sparse regions (most of the tropical Pacific). In relatively data dense areas we should not expect large differences. Velocity potential differences are more widespread, the data network in the tropics is rarely dense enough to define the divergent wind field and so the first guess divergence is often left largely unchanged.

It is interesting to look at the differences between the diagnosed heating and control assimilations cycle by cycle (smoothed using the Sardeshmukh and Hoskins (1984) spectral filter). Fig 10 shows the 200 hPa streamline differences (contours are isotacs). Differences initially occur in the central and western Pacific, and to a lesser extent, over Indonesia. These differences grow in the areas of convective heating and extend both westwards and eastwards through advection, becoming largest in the eastern Pacific. By 12 UTC on 2/2/87 differences of over 5 m s^{-1} are not uncommon. Impact of the change is gradual, and increases with the length of the assimilation. Differences remain largely confined to relatively data sparse areas, as would be expected.

There are large differences between the two assimilations. In order to determine which is most representative of the real atmosphere the rms difference between fields and radiosonde observations has been calculated and averaged for all the observations available within the tropical belt 20°N to 20°S , for each of the eight cycles. These rms values have then been averaged over the eight cycles. Fig 11 shows the fit of the fields to the observations. There is hardly any impact on the fit of the wind field to observations in either the initialised analyses or the first guess fields, except at 100 hPa where the control seems slightly better. For the geopotential the diagnosed assimilation fits the observations more closely below 150 hPa, although the initialised analysis seems worse at 100 hPa. Interestingly the difference at 100 hPa is not carried over into the first guess forecasts, which are of much the same quality in this respect. Where conventional data is available the analyses are constrained by the data to be similar. As significant analysis differences are therefore confined to areas in which conventional data is sparse it is difficult to verify the analyses in these regions using conventional data.

ENSEMBLE DIFFERENCE BETWEEN DIAGNOSED HEATING AND CONTROL ASSIMILATIONS

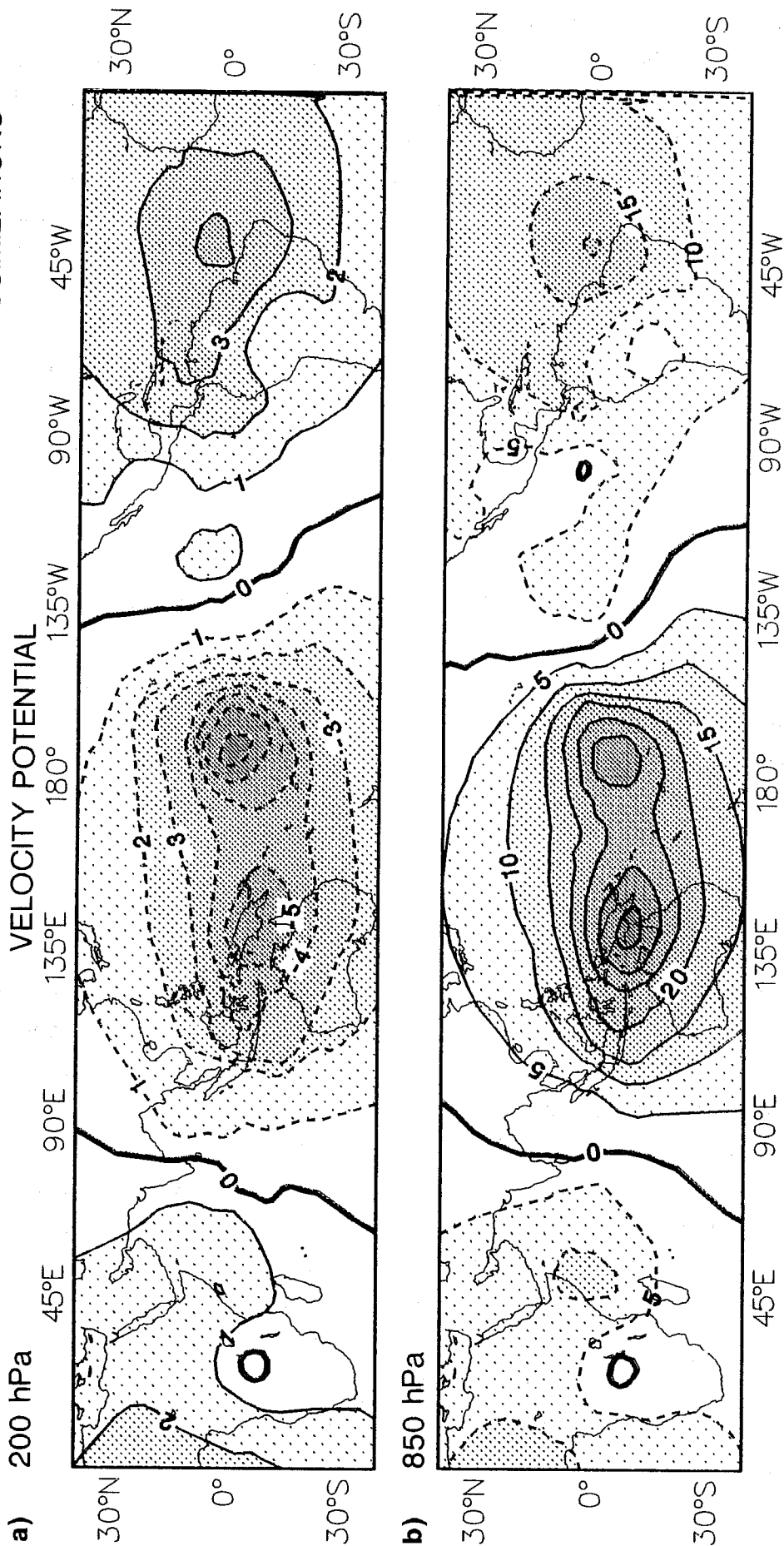


Fig 8. Ensemble difference between diagnosed heating and control assimilations (7 cycles). Velocity potential field a) 200 hPa, contour interval $10^6 \text{ m}^2 \text{ s}^{-1}$; b) 850 hPa, contour interval $5 \times 10^5 \text{ m}^2 \text{ s}^{-1}$. Negative values dashed.

ENSEMBLE DIFFERENCE BETWEEN DIAGNOSED HEATING AND CONTROL ASSIMILATIONS

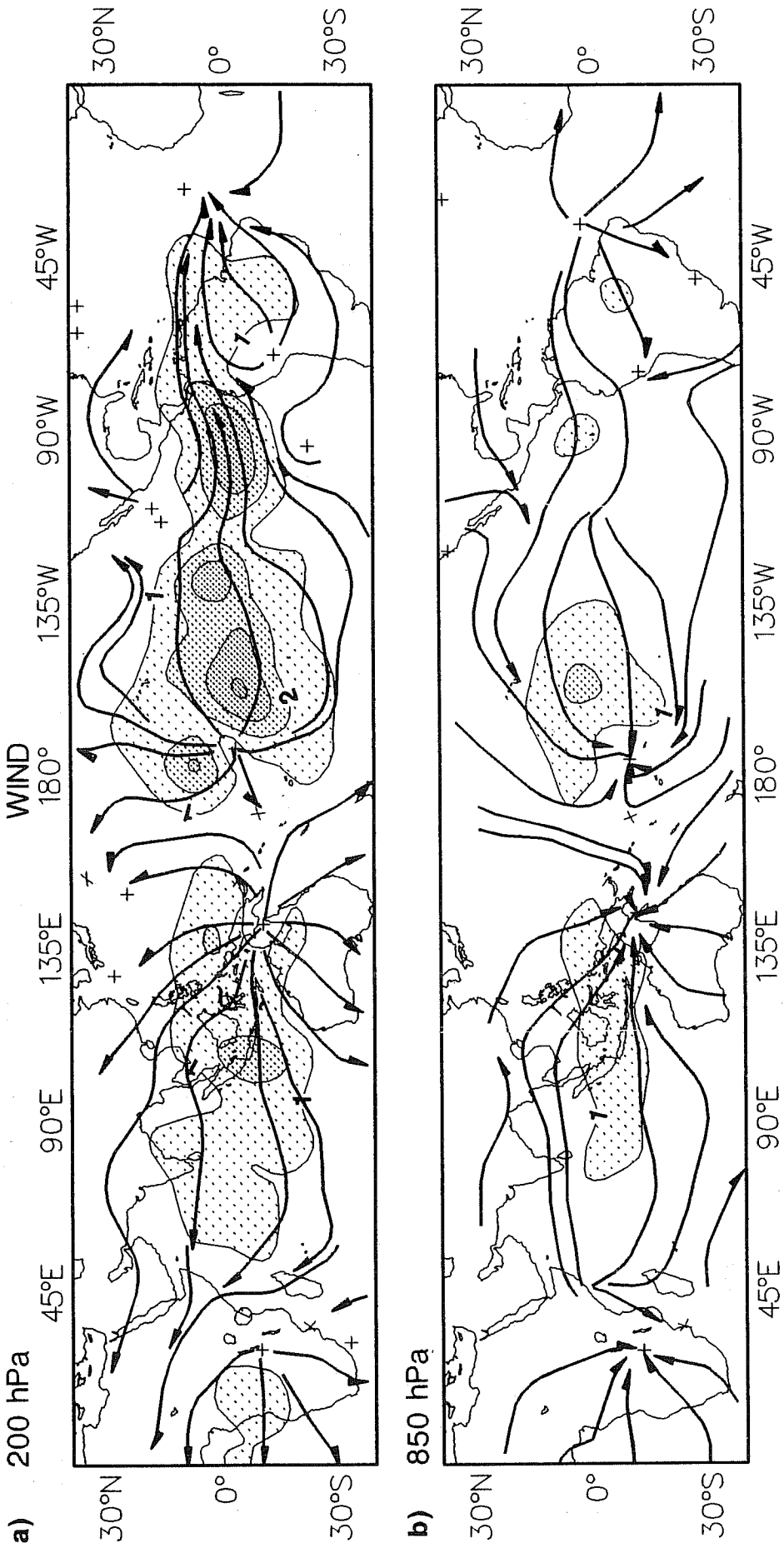


Fig 9. Ensemble difference between diagnosed heating and control assimilations (7 cycles). Streamlines, contours are isotacs. a) 200 hpa, b) 850 hPa. Contour interval 1 ms⁻¹.

DIFFERENCE BETWEEN DIAGNOSED HEATING AND CONTROL ASSIMILATIONS

200 hPa WIND

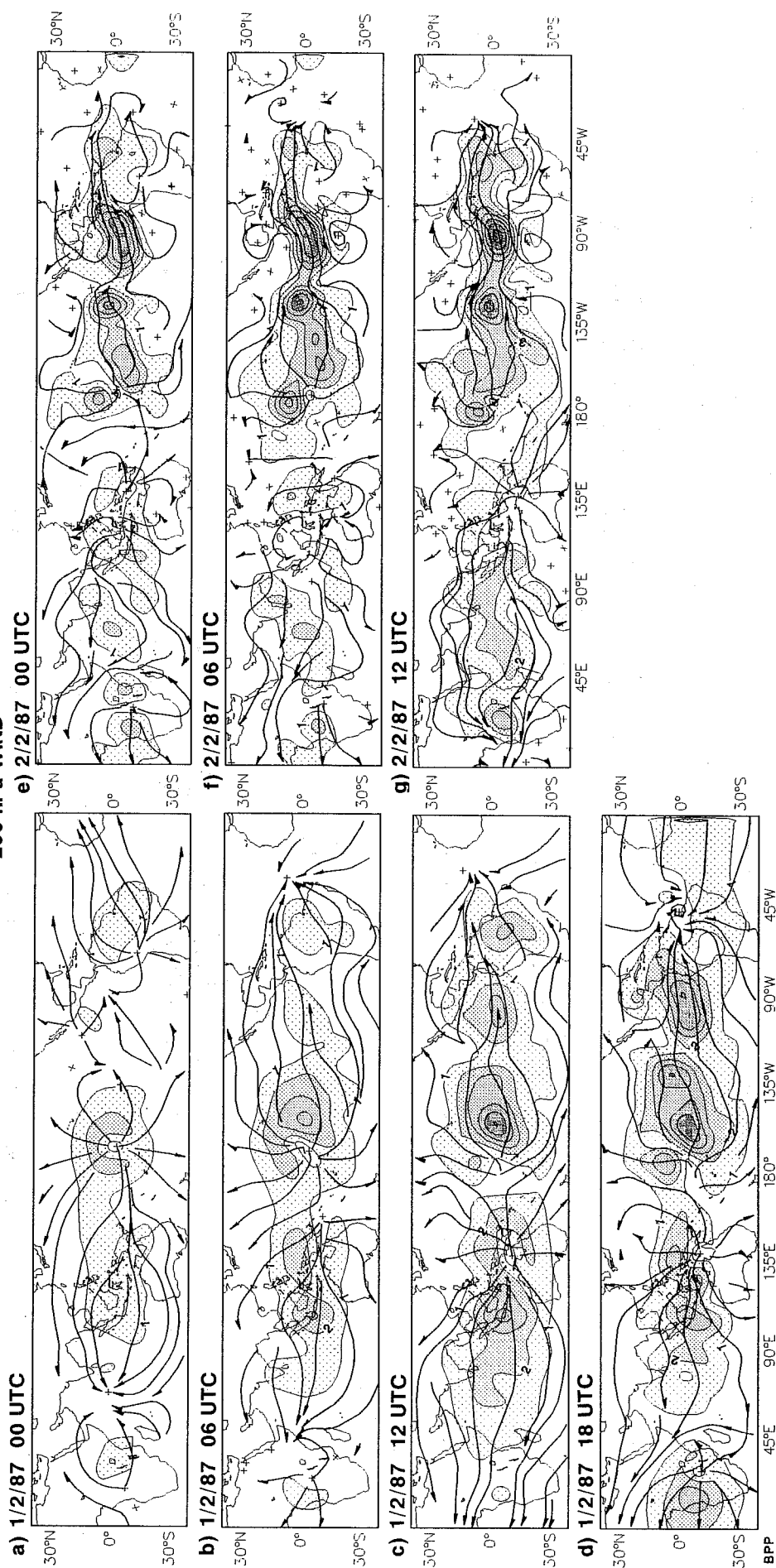


Fig 10. Difference between diagnosed heating and control assimilations cycle by cycle. 200 hPa streamlines, contours are isotacs at interval 1 ms⁻¹. Fields are smoothed using the Sardeshmukh and Hoskins (1984) spectral filter.

A second assimilation has been carried out over the period 00 UTC on 1/2/87 through to 12 UTC on 2/2/87. In this case, in addition to using the diagnosed heating in the initialization it has also been used during the first guess forecasts, with the weights modified by a time factor

$$1., \quad t \leq 2.5 \text{ hours}$$

$$(6 - t)/3.5, \quad 2.5 > t \leq 6 \text{ hours,}$$

in this way the diagnosed heating is used as before for the first 2 1/2 hours of the forecast, beyond this time spin up is still a problem and therefore the diagnosed heating may be more reasonable than the model produced fields. The weighting is steadily reduced to zero, because it a) it is not reasonable to hold the heating constant for such a length of time, b) to allow the model fields to 'adjust'. Note that the heating is **not** being filtered during the six hour first guess forecasts, only during the initialization. The effect of this modification is to further enhance the differences seen above. Characteristics of the changes are much the same. Quality of the assimilation, in terms of rms fit to radiosonde observations, is slightly degraded.

6. FORECAST IMPACT

Forecast experiments have been carried out from the initial conditions on 12 UTC 2/2/87 from both control and diagnosed heating assimilations. They have been verified against the diagnosed heating assimilation as this extends through to 8/2/87, whilst the control assimilation ends on 2/2/87. Usually forecast differences are much larger than analysis differences and verification against one assimilation rather than the other should not impose too large a handicap.

After twenty four hours the forecast differences are similar to those at the start of the forecast (Fig 10g), but slightly increased in magnitude. This is encouraging as it means that the information is being retained by the forecast model. As the forecast proceeds, these differences, which are initially largest over the central and eastern Pacific and over Indonesia, are steadily spread elsewhere. By ninety six hours differences (shown here smoothed, using the Sardeshmukh and Hoskins (1984) spectral filter) at 200 hPa (Fig 12) are typically about 4 m s⁻¹ throughout the tropics and sub tropics. Poleward of about 40° differences are mainly less than 2 m s⁻¹. Largest differences at this time occur over the equatorial Atlantic and are about 14 m s⁻¹. Despite these seemingly large differences between the forecast fields, due to the large systematic error growth in the tropical forecasts, the two forecasts are more similar to each other than either is to the analysis.

RMS fit to radiosonde observation Tropical Belt 20 N – 20 S

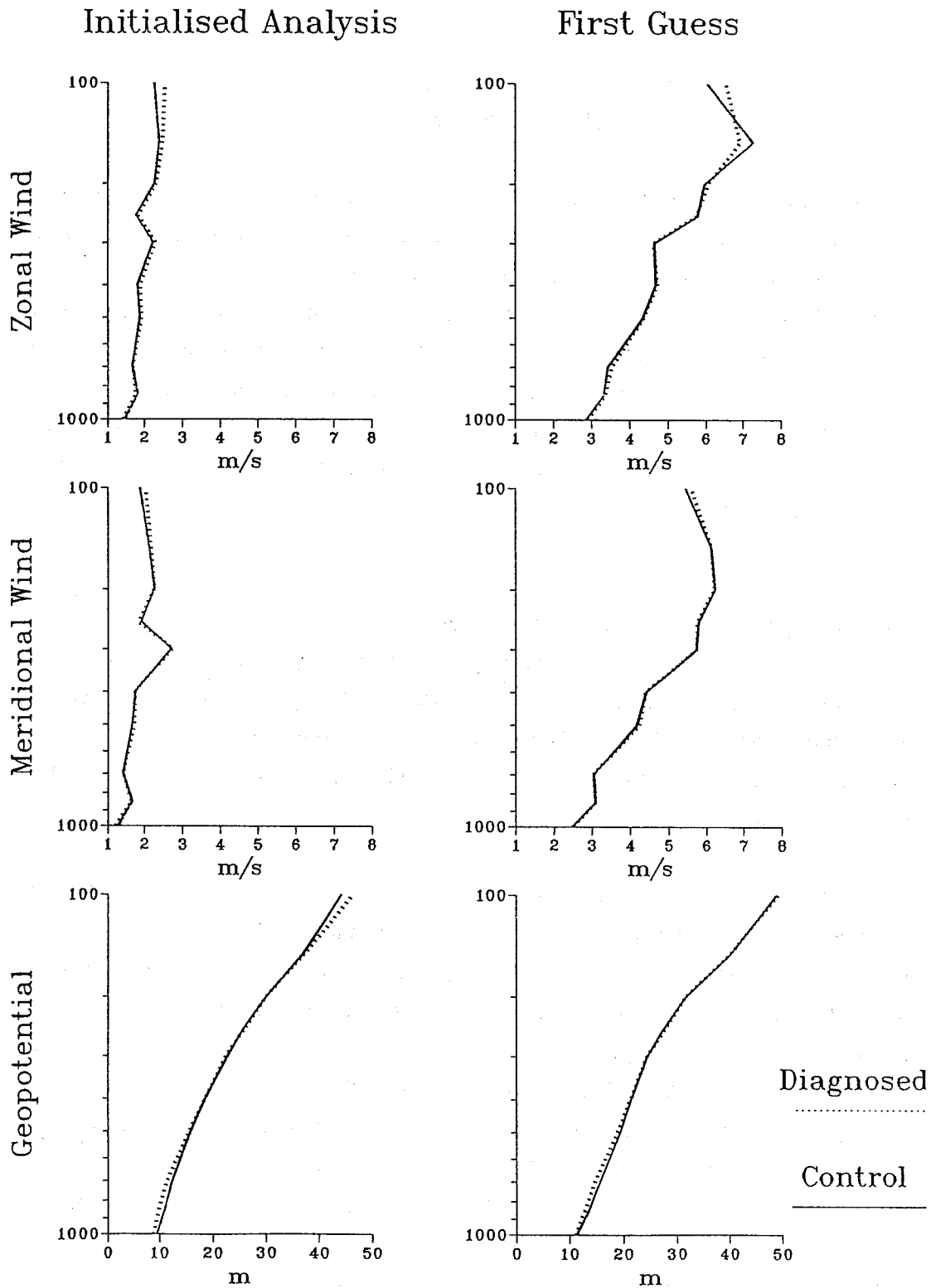


Fig 11.

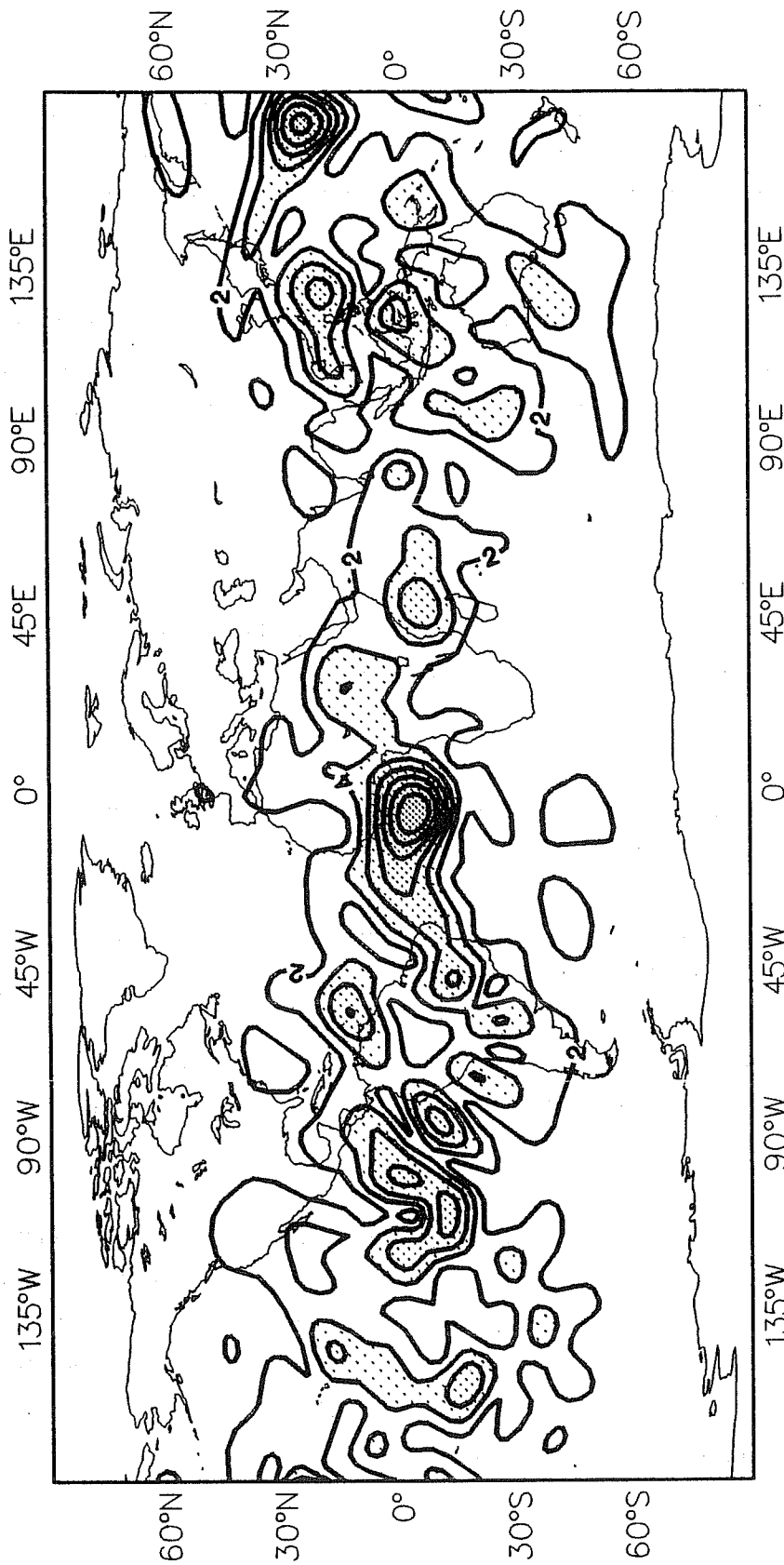


Fig 12. Difference between forecasts from 12 UTC 2/2/87 from the diagnosed heating assimilation and the control assimilation, at 96 hours. 200 hPa streamlines, contours are isotacs at interval 2 ms^{-1} . Fields are smoothed using the Sardeshmukh and Hoskins (1984) spectral filter.

In terms of objective scores the forecast from the diagnosed heating assimilation does better in the tropics, little difference occurs outside the tropics. Improvement is most marked in the long waves.

One should be wary about drawing conclusions from a single forecast, in general a large number of forecasts should be undertaken, in different synoptic situations and seasons. The results shown here can only be taken as indicative that further research is warranted.

7. DISCUSSION

Without doubt the most serious problem for producing analyses of the tropical atmosphere is the lack of conventional data. Maximum use must therefore be made of informational available from meteorological satellites. This, however, only allows determination of the wind at one, or at most, two levels, and rarely are enough cloud track winds processed in order to clearly define the divergence field at either of these levels.

Dominance of diabatic processes within the tropics suggests the utilisation of more direct measures of the diabatic forcing within the assimilation. Use of satellite data to specify heating rates allows their use within the diabatic non linear normal mode initialisation. This not only introduces an additional source of data into the assimilation, it reduces the dependence of the analyses on the assimilating model's parameterization scheme (which is in any case, suffering from spin up problems). Use of diagnosed heating in the assimilation has a large impact, which suggests that the use of this additional data source is important.

Only very crude estimates of the precipitation have been made in this study, and this information has been heavily filtered through the way it is used in the initialization. It should be possible to obtain better estimates of the precipitation, perhaps by taking into account other satellite information (humidity etc). Other instruments, such as SSM/I, will yield more direct and reliable estimates. Use of more reliable data such as this should also allow less filtering to be used in the initialization.

Inclusion of the diagnosed heating through the Kuo scheme is not without its problems. In particular, the tendency of the model to turn off convection over tropical continents at night, and the too stable atmosphere over the tropical Atlantic in the analyses, will require attention. It is not as obvious how to incorporate such diagnosed heating through other convection schemes, such as, for example the Mass Flux scheme (Tiedtke, 1989), which has now replaced the Kuo scheme in the ECMWF operational forecasting model.

In view of the above reservations this should perhaps be considered more as a sensitivity study rather than a definitive guide to initializing tropical forecasts. In this spirit it is clear that the use of diagnosed heating rates in the initialization has a fairly large impact in the analyses in data sparse regions. Evaluation of the quality of the analyses is not easy, but fit to observations suggest that both analysis quality and first guess quality is improved, at least below 150 hPa. Some problems seem to occur above 100 hPa. Forecast impact is also significant and here too a modest improvement is seen.

References

- Arkin, P.A., 1979: The relationship between fractional coverage of high cloud and rainfall accumulations during GATE over the B- scale array. *Mon.Wea.Rev.*, **107**, pp 1382-1387.
- Arkin, P.A. and B.N. Meisner, 1987: The relationship between large-scale convective rainfall and cold cloud over the Western hemisphere during 1982-84. *Mon.Wea.Rev.*, **115**, pp 51-74.
- Barrett, E.C. and D.W. Martin, 1981: The use of satellite data in rainfall monitoring. Academic Press, 340 pp.
- Bengtsson, L., M. Kanamitsu, P. Källberg and S. Uppala, 1982: FGGE 4-Dimensional Data Assimilation at ECMWF. *Bull.A.Met.Soc.*, **63**, pp 29-43.
- Cats, G.J. and W. Wergen, 1983: Analysis of large scale normal modes by ECMWF analysis scheme. ECMWF workshop on current problems in data assimilation. pp 343-372.
- Donner, L.J. 1988: An initialization scheme for cumulus convection in Numerical Weather Prediction Models. *Mon.Wea.Rev.*, **116**, pp 377-385.
- Donner, L.J. and R.J. Rasch, 1990: Cumulus initialization in a global model for numerical weather prediction. *Mon. Wea. Rev.*, To appear.
- Gill, A.E., 1980: Some simple solutions for heat induced circulation. *Quart.J.R.Met.Soc.*, **106**, pp 447 - 462.
- Girard, C. and M. Jarraud, 1982: Short and medium range forecast differences between a spectral and grid point model: An extensive quasi- operational comparison. Tech. Rep. No. 32, ECMWF, 176 pp. Available from ECMWF.
- Gray, W.M. and R.W. Jacobson, 1977: Diurnal variation of deep cumulus convection. *Mon.Wea.Rev.*, **105**, pp 1171- 1187.
- Heckley, W.A., 1985: Systematic errors of the ECMWF operational forecasting model in tropical regions. *Quart.J.R.Met.Soc.*, **111**, pp. 709-738.
- Heckley, W.A. and K. Puri, 1988: The winter monsoon during AMEX. A quick look atlas. Available from ECMWF. 173pp.
- Holland, G.J., J.L. McBride, R.K. Smith, D. Jasper and T.D. Keenan, 1986: The BMRC Australian monsoon experiment: AMEX. *Bull.Amer.Met.Soc.*, **67**, pp 1466-1472.

Hollingsworth, A., 1986: Objective Analysis for Numerical Weather Prediction. Proceedings of the WMO symposium on Numerical Weather Prediction, Tokyo, August 1986.

Hollingsworth, A., D.B. Shaw, P. Lönnberg, L. Illari and A.J. Simmons, 1986: Monitoring of observation and analysis quality by a data assimilation system. *Mon.Wea.Rev.*, **114**, pp 861-879.

Hollingsworth, A., J. Horn and S. Uppala, 1988: Verification of FGGE assimilations of the tropical wind field: the effect of model and data bias. ECMWF Research Department Tech. Memo. No. 145., 43pp. Available from ECMWF.

Jaeger, L., 1976: Monatskarten des Niederschlags für die Ganze Erde. *Berichte Deutschen Wetterd. Offenbach/Main*, **18**, Nr. 139, 38pp.

Jones, D.E., 1976: The United Kingdom Meteorological Office objective analysis scheme for GATE. *Met.Magazine*. Vol **105**, No. 1250. pp 249-260.

Julian, P.R., 1984: Objective analysis in the tropics: A proposed scheme. *Mon.Wea.Rev.*, **112**, 1752-1767.

Källberg, P., 1985: On the use of cloud track wind data from FGGE in the upper troposphere. ECMWF Research Department Tech. Memo. NO. **111**, 39 pp.

Kanamitsu, M., 1985: A study of the predictability of the ECMWF operational forecast model in the tropics. ECMWF Tech. Rep. No. **49**, 73pp.

Kasahara, A., R.C. Balgovind and B.B. Katz, 1988: Use of Satellite Radiometric Imagery Data for Improvement in the Analysis of Divergent Wind in the Tropics. *Mon.Wea.Rev.*, **116**, 866-883.

Krishnamurti, T.N., S. Cocke, R. Pasch and S. Low-Nam, 1983: Precipitation estimates from raingauge and satellite observations summer MONEX FSU Report No. **83-7**, May 1983. 373 pp. Available from Florida State University, Tallahassee, FLA 32306.

Krishnamurti, T.N., T. Kitade and R. Pasch, 1984: Details of low latitude medium range numerical weather prediction using a global spectral model II. Effects of orography and physical initialisation. *J.Meteor.Soc.Japan*, **62**, 613-649.

Krishnamurti, T.N., and S. Low-Nam, 1986: On the Relationship between the Outgoing Long Wave Radiation and the Divergent Circulation. *J.Meteor.Soc.Japan*, **64**, 709- 719.

Krishnamurti, T.N., H.S. Bedi, W. Heckley and K. Ingles, 1988: Reduction of Spinup Time for Evaporation and Precipitation in a Spectral Model. *Mon.Wea.Rev.* **116**, pp. 907-920.

Lorenc, A.C., 1981: A global three-dimensional multivariate statistical interpolation scheme. *Mon.Wea.Rev.*, **109**, pp 701-721.

Lorenc, A.C. and R. Swinbank, 1984: On the accuracy of general circulation statistics calculated from FGGE data - a comparison of results from two sets of analyses. *Q.J.R.Meteorol.Sos.*, **110**, pp 915-942.

Lyne, W.H., R. Swinbank and N.T. 1982: A data assimilation experiment and the andglobal circulation during the FGGE special observing periods. *Quart.J.R.Met. Soc.*, **457**, pp 575 - 594.

- Machenhauer, B., 1977: On the dynamics of gravity oscillations in a shallow water model, with applications to normal mode initialisation. *Beitr.Phys.Atmos.*, **50**, pp 253-271.
- Miller, M.J., T.N. Palmer and R. Swinbank, 1989: Parametrization and Influence of Subgrid Orography in General Circulation and Numerical Weather Prediction Models. *Meteorol.Atmos.Phys.*, **40**, pp 84-109.
- Mohanty, U.C., A. Kasahara, and R. Errico, 1986: The impact of diabatic heating on the initialization of a global forecast model. *J.Meteor.Soc.Japan*, **64**, pp 805- 817.
- Puri, K., 1987: Specification of diabatic heating in the initialization of numerical weather prediction models. ECMWF workshop on Diabatic Forcing pp 151-176
- Richards, F. and P. Arkin, 1981: On the relationship between satellite observed cloud cover and precipitation. *Mon.Wea.Rev.*, **109**, pp 1081-1093.
- Sardeshmukh, P.D. and B.J. Hoskins, 1984: Spatial smoothing on the sphere. *Mon.Wea.Rev.*, **112**, pp 2524-2529.
- Shaw, D.B., 1984: Special Problems of Analysis and Initialisation in the Tropics. Lectures presented at the workshop on limited- area numerical weather prediction models for computers of limited power. Erice, Italy, 1-14 October 1984. Part II. WMO Short- and Medium-Range Prediction Series. No 11, pp 361-378. Available from WMO.
- Shaw, D.B., P. Lönnberg, A. Hollingsworth and P. Undén, 1987: Data assimilation: The 1984/85 revisions of the ECMWF mass and wind analysis. *Q.J.R.Meteorol.Soc.*, **113**, pp 533-566.
- Simmons, A.J., D.M. Burridge, M. Jarraud, C. Girard and W. Wergen, 1989: The ECMWF Medium-Range Prediction Models Development of the Numerical Formulations and the Impact of Increased Resolution. *Meteorol.Atmos.Phys.*, **40**, pp 28-60.
- Smith, W.L., H.M. Woolf, C.M. Hayden, D.Q. Wark and L.M. McMillin, 1979: The TIROS-N Operational Vertical Sounder. *Bull.Am.Meteorol.Soc.*, **60**, pp 1177-1187.
- Smith, W.L., H.M. Woolf, C.M. Hayden, A.J. Schreiner and J.F. Le Marshall, 1984: The Physical Retrieval TOVS Export Package. Technical Proceedings of the first TOVS study conference. Igls, Austria. W.P. Menzel Editor. Cooperative Institute for Meteorological Satellite Studies. University of Wisconsin, USA.
- Tiedtke, M., 1989: A comprehensive massflux scheme for cumulus parameterization in large-scale models. *Mon.Wea.Rev.*, **117**, pp 1777- 1798.
- Tiedtke, M., J-F. Geleyn, A. Hollingsworth and J-F. Louis, 1979: ECMWF model-parametrization of sub-grid scale processes. ECMWF Tech. Report No. 10. 46pp. Available from ECMWF.
- Tiedtke, M., W. Heckley and J. Slingo, 1988: Tropical forecasting at ECMWF: the influence of physical parametrization on the structure of forecasts and analyses. *Q.J.R.Meteorol.Soc.*, **114**, pp 639-664.
- Wergen, W., 1988: The Diabatic ECMWF Normal Mode Initialisation Scheme. *Beitr.Phys.Atmosph.*, **61**, pp 274-302.
- Wergen, W., 1989: Normal mode initialization and atmospheric tides. *Q.J.R.Meteorol.Soc.*, **115**, pp 535-545.

Wergen, W. and W.A. Heckley, 1987: Initialisation. ECMWF Meteorological Training Course Lecture Notes. 72pp. Available from ECMWF.